

PREDICTION OF EARTH ROTATION PARAMETERS WITH THE USE OF RAPID PRODUCTS FROM IGS, CODE AND GFZ DATA CENTRES USING ARIMA AND KRIGING – A COMPARISON

Maciej MICHALCZAK, Marcin LIGAS, Jacek KUDRYS

Department of Integrated Geodesy and Cartography,
Faculty of Geo-Data Science, Geodesy, and Environmental Engineering,
AGH University of Science and Technology, Krakow, Poland

e-mails: mmichalc@agh.edu.pl, ligas@agh.edu.pl, jkudrys@agh.edu.pl

ABSTRACT. Real-time prediction of Earth Orientation Parameters is necessary for many advanced geodetic and astronomical tasks including positioning and navigation on Earth and in space. Earth Rotation Parameters (ERP) are a subset of EOP, consisting of coordinates of the Earth's pole (PM_x, PM_y) and UT1-UTC (or Length of Day – LOD). This paper presents the ultra-short-term (up to 15 days into the future) and short-term (up to 30 days into the future) ERP prediction using geostatistical method of ordinary kriging and autoregressive integrated moving average (ARIMA) model. This contribution uses rapid GNSS products EOP 14 12h from IGS, CODE and GFZ and also IERS final products – IERS EOP 14 C04 12h (IAU2000A). The results indicate that the accuracy of ARIMA prediction for each ERP is better for ultra-short prediction. The maximum differences between methods for first few days of 15-day predictions are around 0.32 mas (PM_x), 0.23 mas (PM_y) and 0.004 ms (LOD) in favour of ARIMA model. The maximum differences of Mean Absolute Prediction Errors (MAPEs) on the last few days of 30-day predictions are 1.91 mas (PM_x), 0.30 mas (PM_y) and 0.026 ms (LOD) with advantage to kriging method. For all ERPs the differences of MAPEs for time series from various analysis centres are not significant and vary up to maximum value of around 0.05 mas (PM_x), 0.04 mas (PM_y) and 0.005 ms (LOD).

Keywords: ARIMA, kriging, polar motion, length of day, Earth Rotation Parameters

1. INTRODUCTION

Earth Orientation Parameters (EOP), i.e., coordinates of the Earth's pole (PM_x, PM_y), celestial pole offsets (dX, dY), and UT1-UTC describe the irregularities in the Earth's rotation. An additional parameter that is the first negative time derivative from the UT1-UTC is the Length of Day (LOD) (Modiri et al., 2020). In this contribution, a subset of EOP, Earth Rotation Parameters (ERP), consisting of Earth's pole coordinates (PM_x, PM_y) and UT1-UTC (LOD) is subject to prediction.

The knowledge of EOP is essential for transformation between celestial reference frame (CRF) and terrestrial reference frame (TRF) (Gambis and Luzum, 2011), which enables precise positioning in space and on the Earth's surface, navigation, time-keeping and positional astronomy.



EOP are determined by space geodetic techniques such as VLBI (Very Long Baseline Interferometry), DORIS (Doppler Orbitography and Radiopositioning Integrated by Satellite), SLR (Satellite Laser Ranging) and GNSS (Global Navigation Satellite System), and are finally combined into a single solution (Petit and Luzum, 2010). This combination of techniques enables to determine polar coordinates with the accuracy of app. 50 μ s or better and 10 μ s in case of LOD (Dick and Thaller, 2020).

Complexity of measuring and data processing involved in EOP determination forces their prediction since it is impossible to obtain them in real-time mode.

The long EOP time series are published with latency by International Earth Rotation and Reference System Service (IERS) and many individual analysis centres or services (IERS Annual Report 2018). Therefore, in operational settings, this gap must be filled with rapid products, e.g., IGS (International GNSS Service), CODE (Center for Orbit Determination in Europe) or GFZ (German Research Centre for Geosciences). This may also be done by basing on rapid products published by IERS, e.g., Daily Rapid EOP Data.

A plenty of prediction methods have been applied to EOP prediction through the years; the following list is by no means exhaustive: least-squares collocation (Hozakowski, 1989), artificial neural networks (Schuh et al., 2002; Liao et al., 2012), autocovariance prediction (Kosek, 2002), autoregression (Kosek et al., 2007), combination of least-squares and multivariate stochastic methods (Niedzielski and Kosek, 2008), wavelets and fuzzy inference systems (Akyilmaz et al., 2011), extreme learning machine (Lei et al., 2015), Gaussian process regression (Lei et al., 2015), combination of least-squares extrapolation and autoregressive modelling of EAM (Dill et al., 2019), singular spectrum analysis (Okhotnikov and Golyandina, 2019), one-step forecasting method based on the LS+AR (Wu et al., 2019), combination of singular spectrum analysis and Copula-based analysis (Modiri et al., 2020) and Kalman filter (Nastula et al., 2020), combination of Holt–Winters algorithm and angular momenta of global surficial geophysical fluids (Luo et al., 2022).

This study is intended in ultra-short-term (up to 15 days into the future) and short-term (up to 30 days into the future) ERP predictions using geostatistical method of ordinary kriging and autoregressive integrated moving average (ARIMA) model. Rapid GNSS products EOP 14 12h from IGS, CODE and GFZ and also IERS final products (IERS EOP 14 C04 12h(IAU2000A)) are used and the results are compared. For all the time series and data centres the first ERP prediction was made for 1 January 2017 (MJD 57754.5) and the last for 15 April 2022 (MJD 59684.5) with 1 day shift.

2. METHODOLOGY

2.1. Statistical agreement between final IERS and rapid CODE, IGS and GFZ products

This section attempts to statistically examine the agreement between ERP final products delivered by IERS and rapid ones delivered by CODE, IGS and GFZ. To accept or reject a hypothesis of equality, for a particular ERP in pairwise combinations of data centres, three techniques are used, i.e., matched-pair t-test, Deming regression (DR), and Passing-Bablok regression (PBR). The mentioned techniques are frequently applied in method comparison studies (e.g., in medicine or clinical chemistry) to search for biases/differences (constant/fixed or proportional) between two measurement methods (or measuring devices). In this contribution, a single pair of ERP coming from IERS (reference) and one of three (IGS, CODE, GFZ) centres on a given MJD is considered as a measurement pair. Matched-pair t-test evaluates whether the differences between variables representing two measurement methods are statistically different from a given constant (to test for equality the constant is

zero); hence it is able to detect only a constant bias. The other two methods quantify and assess deviations from the line of equality (perfect agreement between measurements X and Y given by different methods or devices), i.e.,

$$Y = X \quad (1)$$

by fitting a straight line,

$$Y = aX + b \quad (2)$$

Hence, they are able to detect both fixed (intercept = b) and proportional (slope = a) biases. Deming regression is a method of fitting a straight line to scattered 2D data in an errors-in-variables framework, i.e., both the explanatory variable X and the response variable Y in (2) are considered to be erroneous. In DR, it is assumed that the variance ratio of the measurement errors λ in X and Y is constant; for $\lambda = 1$, DR yields the same results as orthogonal regression (in this study, this assumption was adopted). To assess statistical significance of slope and intercept, a pair of hypotheses is tested, i.e., $H_0: a = 1$ vs. $H_1: a \neq 1$ and $H_0: \text{mean } Y - \text{mean } X = 0$ vs. $H_1: \text{mean } Y - \text{mean } X \neq 0$ to decide whether methods may be considered as equivalent (Linnet 1990).

Passing - Bablok regression is another technique of testing agreement and detecting a potential systematic bias between methods. It is a non-parametric and robust regression method where a slope a in (2) is the median of all slopes computed between any two points excluding cases of $a = 0$ or $a = \text{inf}$ and an intercept b in (2) is calculated as $b = \text{median}(y_i - a x_i)$. For both parameters, the $1-\alpha$ (usually 0.95) confidence intervals (CI) are inferred. If 0 is within the CI of b , and 1 is included in the CI of a , then according to Passing and Bablok (1983), one may infer that $Y = X$ and the two methods are comparable. On the other hand, if 0 is not in the CI of b , there is a systematic difference (bias), and if 1 is not in the CI of a , then there is a proportional difference (bias) between the two methods.

Table 1. Matched-pair t – test between final IERS and rapid CODE, IGS and GFZ ERP products

	ERP	Mean difference [“ / s]	CI lower limit [“ / s]	CI upper limit [“ / s]	Decision
IERS-CODE	PM _x	-0,00002657	-0,00002828	-0,00002486	Reject
	PM _y	-0,00000364	-0,00000493	-0,00000234	Reject
	LOD	-0.00000790	-0.00000829	-0.00000751	Reject
IERS-IGS	PM _x	-0,00001092	-0,00001240	-0,00000945	Reject
	PM _y	-0,00000896	-0,00000996	-0,00000796	Reject
	LOD	0.00000006	-0.00000021	0.00000034	Accept
IERS-GFZ	PM _x	-0,00000536	-0,00000719	-0,00000353	Reject
	PM _y	-0,00002593	-0,00002780	-0,00002406	Reject
	LOD	-0.00001515	-0.00001561	-0.00001468	Reject

*Confidence level $1 - \alpha = 0.95$ for CI

Table 2. Deming regression, final IERS vs rapid CODE, IGS and GFZ ERP products

	ERP	Slope	Intercept [“ / s]	Decision
IERS-CODE	PM _x	1.00003832 t = 3.04479892; p = 0.00235965 (R)	0.00002657 t = 30.52319805; p = 0.00000000 (R)	Reject
	PM _y	0.99999094 t = -0.89663540; p = 0.37002469 (A)	0.00000364 t = 5.50072407; p = 0.00000004 (R)	Reject (partially satisfied)
	LOD	1.00089118 t = 3.15274029; p = 0.00164218 (R)	0.00000790 t = 39.80528652; p = 0.00000000 (R)	Reject
IERS-IGS	PM _x	0.99998689 t = -1.17060095; p = 0.24190291 (A)	0.00001092 t = 14.52462344; p = 0.00000000 (R)	Reject (partially satisfied)
	PM _y	0.99996457 t = -4.60782629; p = 0.00000433 (R)	0.00000896 t = 17.59538975; p = 0.00000000 (R)	Reject
	LOD	1.00020499 t = 1.16628098; p = 0.24364414 (A)	-0.00000006 t = -0.46240588; p = 0.64384211 (A)	Accept
IERS-GFZ	PM _x	1.00008012 t = 5.82033049; p = 0.00000001 (R)	0.00000536 t = 5.74191721; p = 0.00000001 (R)	Reject
	PM _y	1.00006274 t = 4.07633940; p = 0.00004760 (R)	0.00002593 t = 27.24852927; p = 0.00000000 (R)	Reject
	LOD	0.99916958 t = -2.62639779; p = 0.00869725 (R)	0.00001515 t = 63.59095306; p = 0.00000000 (R)	Reject

*Significance level $\alpha = 0.025$ for hypothesis testing; (R), (A) denote Reject or Accept (no ground to reject) in separate hypothesis testing for significance of either a slope or an intercept; decision in the last column concerns the overall hypothesis of equivalence of methods; t is the value of t-statistics which take the form: (slope) $t = (a - 1)/SE(a)$ and (intercept) $t = (\text{mean } Y - \text{mean } X)/SE(\text{mean } Y - \text{mean } X)$ where the standard errors (SE) were calculated using the jackknife method, p is a p-value, when less than adopted $\alpha = 0.025$ then it indicates strong evidence against the null hypothesis.

Table 3. Passing-Bablok regression, final IERS vs rapid CODE, IGS and GFZ ERP products

	ERP	Slope (a / CI)	Intercept (b / CI) [$^{\circ}$ / s]	Decision
IERS-CODE	PM _x	1.0000432 (1.00002075; 1.00006572) (R)	0.0000170 (0.00001399; 0.00001988) (R)	Reject
	PM _y	1.00000000 (0.99997632; 1.00001322) (A)	0.00000200 (-0.00000264; 0.00001059) (A)	Accept
	LOD	1.00100267 (1.00045893; 1.00155259) (R)	0.00000759 (0.00000738; 0.00000778) (R)	Reject
IERS-IGS	PM _x	0.99999126 (0.99997446; 1.00000467) (A)	0.00000545 (0.00000385; 0.00000720) (R)	Reject (partially satisfied)
	PM _y	0.99996812 (0.99995422; 0.99998202) (R)	0.00001770 (0.00001268; 0.00002273) (R)	Reject
	LOD	1.00029612 (1.00000000; 1.00063857) (A)	-0.00000018 (-0.00000026; -0.00000010) (R)	Reject (partially satisfied)
IERS-GFZ	PM _x	1.00006766 (1.00004284; 1.00009256) (R)	-0.00000174 (-0.00000476; 0.00000115) (A)	Reject (partially satisfied)
	PM _y	1.000052582 (1.00002540; 1.00008007) (R)	0.00000175 (-0.00000836; 0.00001128) (A)	Reject (partially satisfied)
	LOD	0.99948267 (0.99882881; 1.00013364) (A)	0.00001554 (0.00001524; 0.00001582) (R)	Reject (partially satisfied)

*Confidence level $1 - \alpha = 0.95$ for CI; (R), (A) denote Reject or Accept (no ground to reject) in separate hypothesis testing for significance of either a slope or an intercept; decision in the last column concerns the overall hypothesis of equivalence of methods

Although the Passing-Bablok regression gives uncertain results (but very close to overall acceptance), the remaining two methods indicate statistically significant agreement (no biases) for the pair IERS-IGS in case of LOD time series, thus they may be considered as equivalent. This will be also visible when results of forecasts will be exposed. On the other hand, Passing-Bablok regression accepts hypotheses of complete agreement (no proportional and fixed biases) for the pair IERS-CODE in case of PM_y; Deming regression accepts only H₀ for the slope ($a = 1$) and rejects H₀ for the intercept, hence fixed bias may be present. The value of the intercept agrees with the bias (mean difference) estimated for the matched-pair t-test. For the remaining pairs of data centres and ERPs, the methods detect either both proportional and fixed biases (rejection of two hypotheses) or either of the two. Despite the detection of differences between products belonging to IERS and considered data centres, it is worth noting that easily interpretable fixed biases (shifts) are of the order of accuracy in determining the Earth's Rotation Parameters. Thus, so far, they may be considered insignificant when confronted with the accuracy of the forecast. In addition, the results may depend on the analysed time span 1 January 2017 (MJD 57754.5) – 15 April 2022 (MJD 59684.5).

2.2. Solid Earth tides

The LOD time series includes periodic effects such as the impact of solid Earth tides with periods varying from 5 days up to 18.6 years. These tidal effects were first removed from

LOD time series by using a model recommended by IERS Conventions (2010) (Petit and Luzum, 2010) which is given by

$$\begin{cases} dLOD = \sum_{i=1}^{62} B'_i \cos \xi_i + C'_i \sin \xi_i \\ \xi_i = \sum_{j=1}^5 a_{ij} \alpha_j \end{cases} \quad (3)$$

where: values of B'_i , C'_i , a_{ij} , and α_j are given in Chapter 8 of the IERS Conventions (2010) (Petit and Luzum, 2010).

2.3. Time – frequency analysis

In order to determine the number of periodic components in the prediction model, a time-frequency analysis of the length-of-day and polar motion time series based on IERS EOP 14 C04 12h (IAU2000A) was performed. Continuous Wavelet Transform with Morlet wavelets was used for this purpose with a time span of approx. 22 years (MJD 51544.5 – 59684.5). In case of LOD, the analysis resulted in a spectrogram with clearly visible lines corresponding to three periods of 0.5, 1 and 8.3 years (Figure 1). Several weaker components of periods between 3.5 and 5.5 years ($5e-4$ 1/day, $8e-4$ 1/day) with increasing amplitude over time are also evident. Signals with lower frequencies visible on the spectrogram were treated as artefacts due to the length of the analysed time interval (22 years) and were not included in the prediction model.

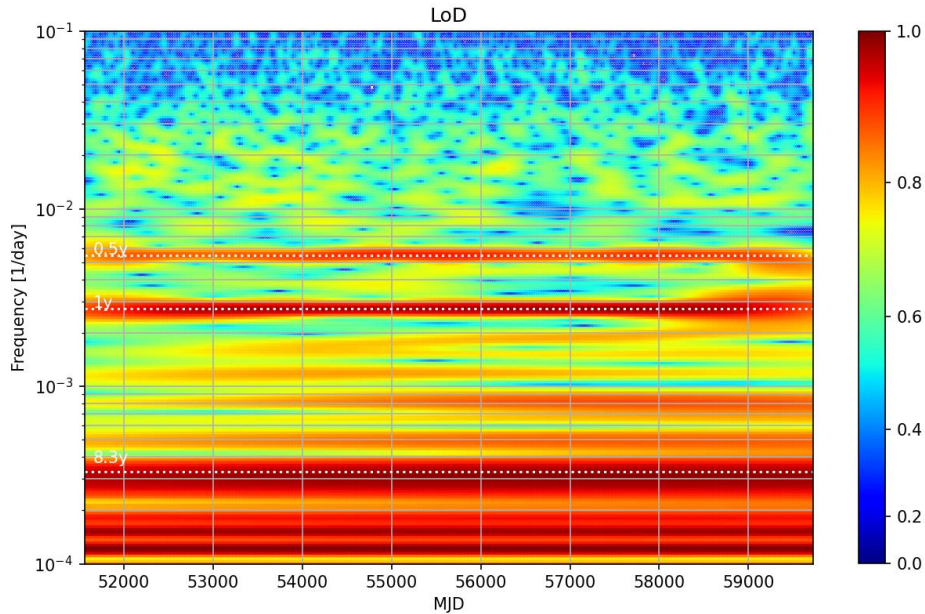


Figure 1. Spectrogram for LOD

The PMx and PMy time series were analysed in a similar manner, obtaining spectrograms with apparent domination of two components with periods of 366 and 431 (annual and Chandler oscillations). Starting at around 57000 MJD, the second component shows decreasing amplitude in both the PMx and PMy series (Figures 2 and 3). A similar effect has been observed previously around 1920-1930 and connected with the Chandler wobble phase change (Zotov and Bizouard, 2018).

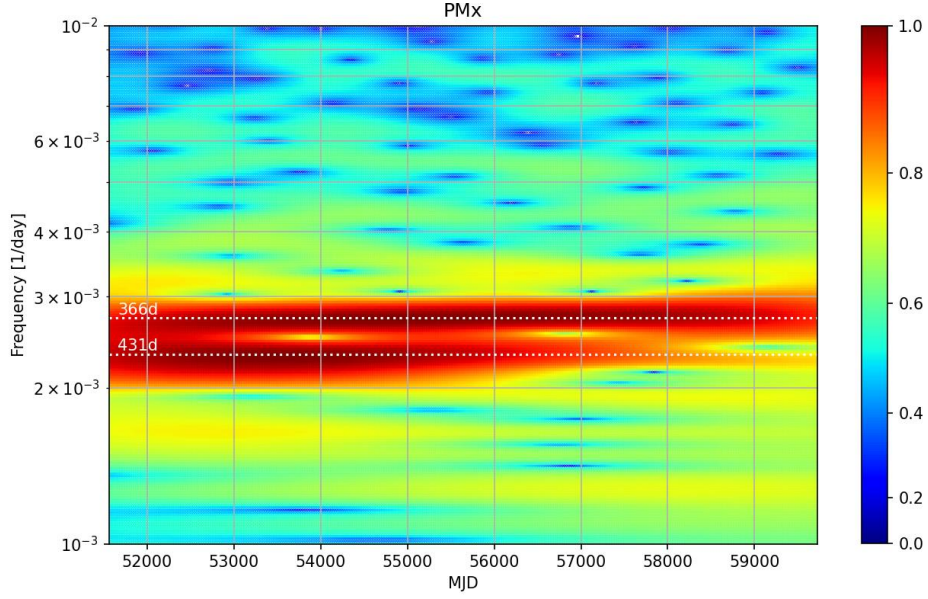


Figure 2. Spectrogram for PMx

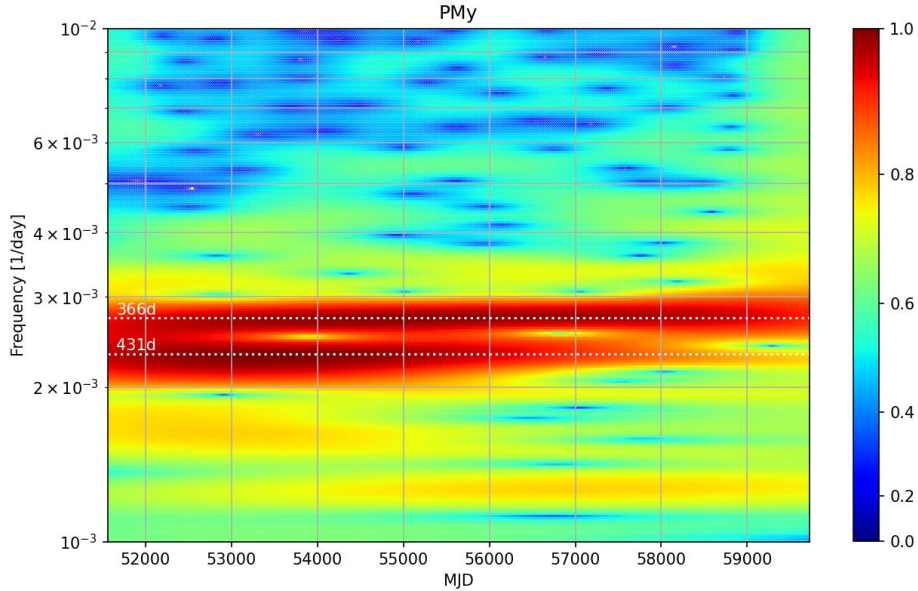


Figure 3. Spectrogram for PMy

2.4. Prediction model

Both LOD and pole coordinates are decomposed into linear and periodic components. The prediction model consists of mentioned components (extrapolated into the future) and residuals (obtained in the prediction process), and is given as follows:

$$\widehat{ERP}(t_p) = \hat{a}_0 + \hat{a}_1 t_p + \sum_{i=1}^n \hat{b}_i \sin(\hat{c}_i t_p + \hat{d}_i) + [dLOD] + \hat{\varepsilon}(t_p) \quad (4)$$

where \widehat{ERP} is a predicted ERP; t_p is the prediction time moment; \hat{a}_0, \hat{a}_1 are the estimated linear trend coefficients; n is the number of terms in the series; $\hat{b}_i, \hat{c}_i, \hat{d}_i$ are the estimated amplitudes, frequencies, and phase constants for i -th sine term, respectively; $dLOD$ are tidal corrections (occur only in LOD prediction) and $\hat{\varepsilon}$ stands for the predicted residual.

2.5. Ordinary kriging

Ordinary kriging, adapted to time series prediction herein, is a linear predictor of an unknown random quantity Z at a time instant t_0 (here residual PM and LOD processes), i.e.,

$$\hat{Z}(t_0) = \boldsymbol{\lambda}^T \mathbf{Z}(t) \quad (5)$$

where $\mathbf{Z}(t)$ are observed data.

It is optimal, in the sense of Best Linear Unbiased Prediction – BLUP (and Best Linear Unbiased Estimator – BLUE), if the mean value of a random process is an unknown constant (Cressie, 1993). Unknown mean value is eliminated from the prediction procedure by unbiasedness condition of summing up weights to unity, i.e., $\boldsymbol{\lambda}^T \mathbf{u} = 1$, and is internally estimated from the sample (Ligas, 2022). Optimal coefficients $\boldsymbol{\lambda}$ (kriging weights), in the sense of unbiasedness and minimization of mean squared prediction error, are computed from the system of equations:

$$\begin{bmatrix} \boldsymbol{\Omega} & \mathbf{u} \\ \mathbf{u}^T & 0 \end{bmatrix} \begin{bmatrix} \boldsymbol{\lambda} \\ \kappa \end{bmatrix} = \begin{bmatrix} \boldsymbol{\omega}_0 \\ 1 \end{bmatrix} \quad (6)$$

where $\boldsymbol{\Omega}$ is a covariance matrix of observations (observations – observations), $\boldsymbol{\omega}_0$ stands for a covariance vector between observations and a target location to be predicted (observations – prediction), and \mathbf{u} is a vector of ones.

Additional unknown κ (Lagrange multiplier) in (6) results from the unbiasedness condition. Ordinary kriging offers a measure of prediction quality (minimized mean squared prediction error σ_{OK}^2) which may be expressed as

$$\sigma_{OK}^2 = \sigma^2 - \boldsymbol{\lambda}^T \boldsymbol{\omega}_0 - \kappa \quad (7)$$

where σ^2 is a variance of observations.

Kriging is a two-step procedure. Firstly, the temporal structure of a random process is inferred (from data and a priori knowledge if available) and contained in a semivariance or covariance function. Then, the covariance structure stored in $\boldsymbol{\Omega}$ and $\boldsymbol{\omega}_0$ is employed to solve for kriging weights in (6) and to assess the quality of prediction in (7).

2.6. ARIMA

This study also uses autoregressive integrated moving average (ARIMA) model, which is the combination of autoregressive model, moving average model, and differencing process (integrated part). This model makes possible to obtain greater flexibility in fitting the model to the actual time series (Box and Jenkins, 1976). The model mentioned above can be applied not only on a stationary time series but also on series that behave in a non-stationary way. In order to check the stationarity of the time series, the Kwiatkowski–Phillips–Schmidt–Shin (KPSS) test was used (Kwiatkowski et al., 1992). ARIMA model is defined as follows (Box and Jenkins, 1976):

$$\hat{X}_t^d = c + \sum_{i=1}^p \varphi_i X_{t-i}^d + \sum_{i=1}^q \theta_i \varepsilon_{t-i} + \varepsilon_t \quad (8)$$

where X_t^d is the predicted value; c is a constant; p is the order of autoregressive process; $\varphi_1 \dots \varphi_p$ are parameters of the model; d is the degree of differencing; X_{t-i}^d are the differenced past series values; q is the order of moving average process; $\theta_1 \dots \theta_q$ are parameters of the model; ε_{t-i} are the past white noise error terms; and ε_t is the white noise.

ARIMA model is generally denoted as ARIMA (p, d, q).

3. DATA DESCRIPTION AND PROCESSING

In this contribution, rapid EOP 14 12h (IGS, CODE, and GFZ) and final EOP 14 C04 12h (IERS) daily products were used to predict ERP. The obtained predictions cover the time interval from 1 January 2017 (MJD 57754.5) to 15 April 2022 (MJD 59684.5) for all evaluated ERP time series/data centres.

Prediction procedure is based on that one described in Michalczak and Ligas (2021) and Michalczak and Ligas (2022) set of parameters such as the number of the nearest neighbors (NN) for kriging, number of observations for structure function estimation, the time span (TS) necessary to estimate parameters of a linear trend and number of periodic components. The TS parameter for PM_x and PM_y is equal to 6.4 yrs and for LOD 9.2 yrs; NN for PM_x and PM_y equals to 10 immediate neighbors and for LOD it is equal to 25.

In case of ARIMA(p, d, q) model, the best set of parameters p and q was obtained by means of corrected Akaike Information Criterion (AICc) (Akaike, 1998). The loop with AICc criterion was run over the number of p and q varying from 1 to 5; the best set of parameters was selected and then a prediction was made based on them. For each 15-day and 30-day ERP prediction, the best set of p and q was selected separately. Parameter d determines a degree of differencing to be applied in order to transform a non-stationary time series into the stationary one in the mean sense. Stationarity of each ERP time series was checked using the KPSS test. Pole coordinates time series (after removing components mentioned in 2.4.) passed the stationary test for $d = 2$ and for LOD time series (after removing components mentioned in 2.2. and 2.4.) $d = 1$.

The prediction process starts with the selection of the first day of forecast. Then, the 30 observations preceding the first day of forecast were selected (rapid products from CODE, GFZ or IGS), while further back observations were taken from the final product (IERS). Afterward, the ERP predictions were carried out with ARIMA model and kriging for 15 and 30 days ahead. Obtained results were compared with each ERP IERS final time series. The whole process is then repeated, shifting the first day of prediction to next day and repeated until the last day of the forecast is reached, i.e., 15 April 2022. The process is illustrated in Figure 4. The prediction process based on final product (IERS) did not use any rapid products (this is to compare results of prediction with and without rapid product supplementation), which means that the 30 observations preceding the first day of prediction were selected from the final product – IERS EOP 14 C04 12h.

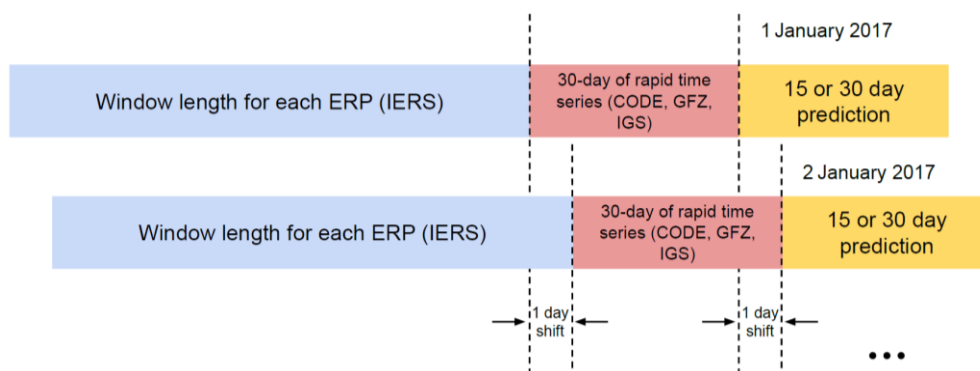


Figure 4. Diagram of the whole prediction process with rapid products

For the IGS, GFZ, and IERS, the total number of 15-day predictions for each ERP and each method amounts to 1886 and the total number of 30-day predictions is equal to 1871. Due to gaps in the CODE time series, the number of each ERP forecasts is equal to 1822 and for 30-day predictions amounts to 1807.

4. RESULTS

The ERP prediction accuracy was assessed by means of the mean absolute prediction error (MAPE) given by

$$MAPE_j = \frac{1}{n} \sum_{i=1}^n |e_{i,j}| \quad j := \text{prediction day number} \quad (9)$$

where n is a number of predictions, $e_{i,j} = O_{i,j} - P_{i,j}$ is the prediction error, O stands for observed and P for predicted ERP.

Figure 5 and 6 present the values of MAPEs for ultra-short (15-day into the future) PMx and PMy prediction using ARIMA and kriging for data time series from four analysis centres.

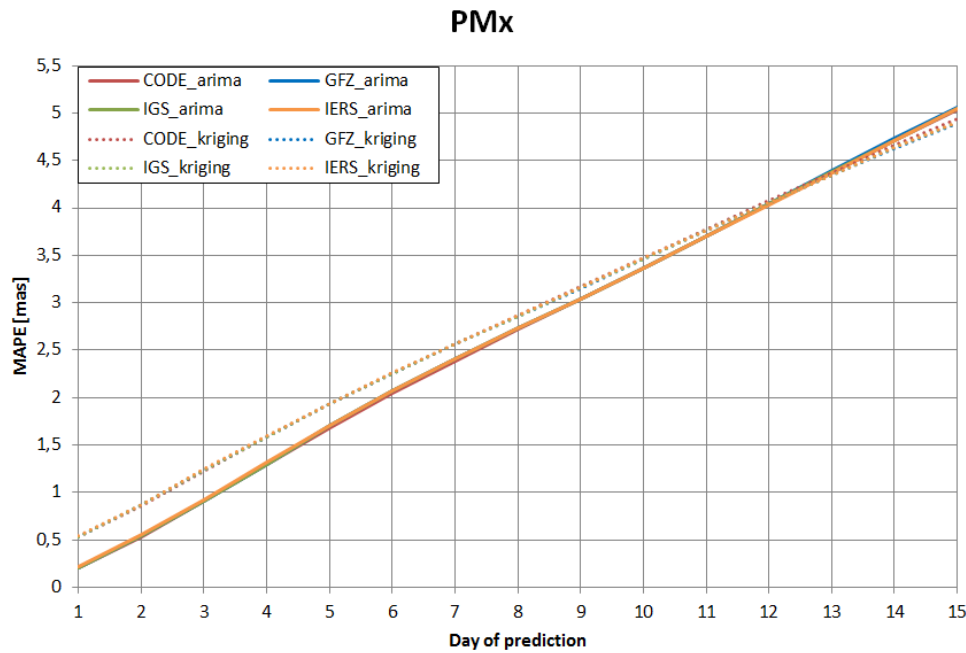


Figure 5. Comparison of MAPEs for 15-day PMx prediction for ARIMA and kriging for various analysis centres (CODE, GFZ and IGS denote rapid time series and IERS final time series)

PMx prediction with ARIMA model offers better accuracy up to day 13; after this day the advantage is on the side of kriging. For the first 5 days, the advantage is around 0.3 mas in favour of the ARIMA model. As the forecast day increases, the difference between ARIMA model and kriging decreases. For the 15th day, the difference is around 0.15 mas in favour of kriging. MAPEs for PMx for each analysis centres are very similar. The average difference between MAPEs for PMx prediction with ARIMA model is around 0.01 mas. In case of kriging, prediction performance is similar, but only for first 10 days. Then, MAPEs for CODE time series increase and differ from the other centres by about 0.04 mas.

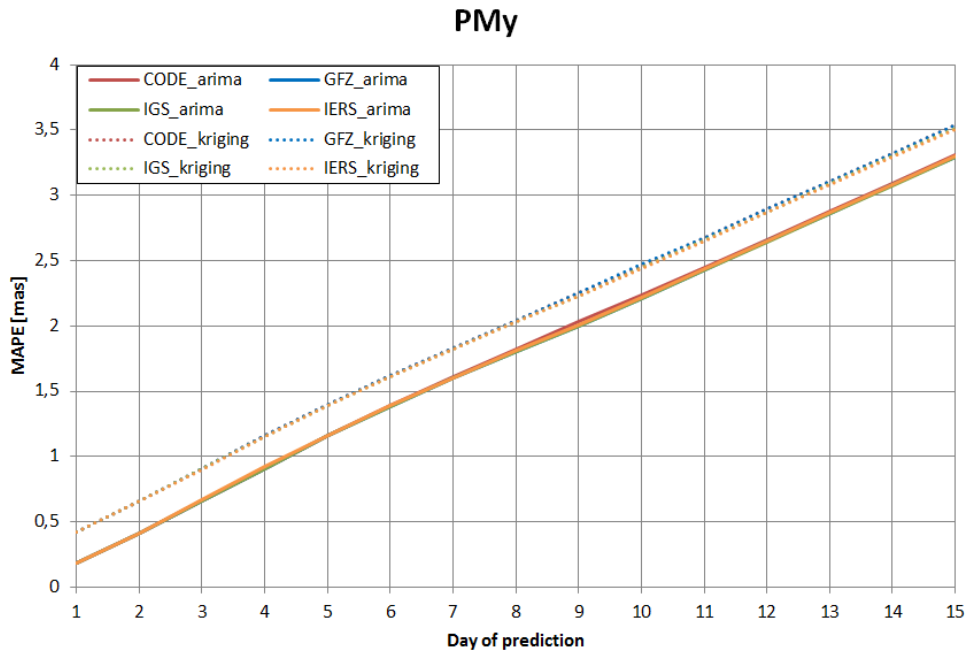


Figure 6. Comparison of MAPEs for 15-day PMy prediction for ARIMA and kriging for various analysis centres

PMy prediction with ARIMA model offers better accuracy up to the last day. The differences between ARIMA and kriging are around 0.23 mas in favour of ARIMA. Similarly to PMx results, the average difference between MAPEs for PMy prediction with ARIMA for four centres is around 0.01 mas with maximum value 0.03 mas. MAPEs for various centres for kriging prediction up to 8th day of prediction are nearly the same (with difference around 0.01 mas). On the 9th day of prediction differences between various centres increase to 0.02 mas and then on the last day, they reach values around 0.04 mas.

For both PMx and PMy, prediction accuracy based on final data (IERS) does not differ significantly from accuracy obtained with rapid products (CODE, GFZ and IGS) supplementing. This insignificant difference between the forecasts based on either final or rapid data applies also to 30-day predictions of PMx/PMy and to both LOD forecast horizons.

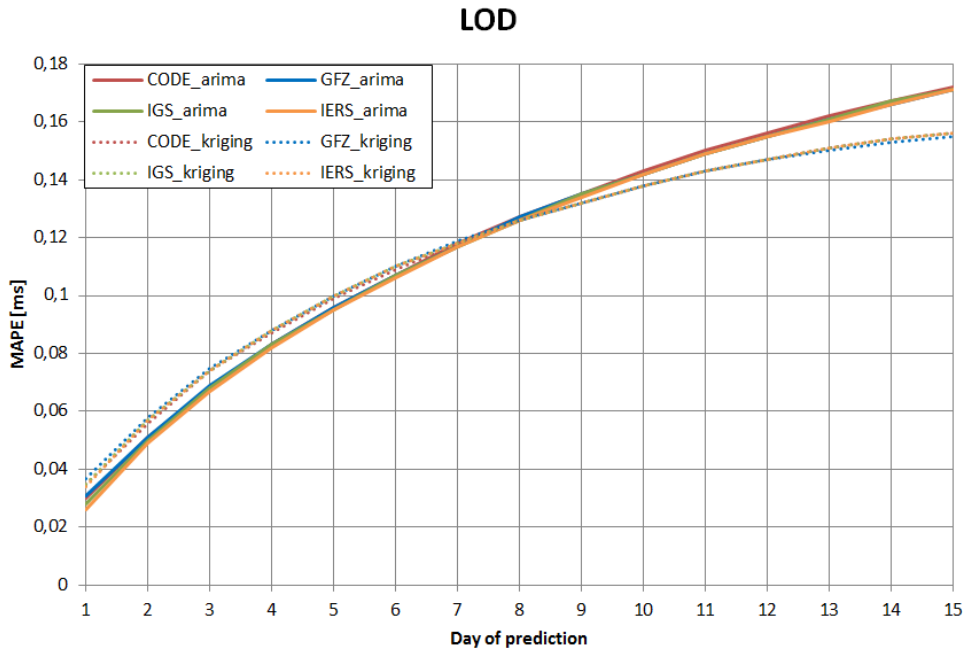


Figure 7. Comparison of MAPEs for 15-day LOD prediction for ARIMA and kriging for various analysis centres

Figure 7 presents the values of MAPEs for ultra-short (15-day into the future) LOD prediction using ARIMA and kriging for time series from four analysis centres. For the first 7 days, lower values of MAPEs are obtained, with advantage around 0.004 ms, for ARIMA. After this day, the advantage is on the side of kriging with maximum difference equal to about 0.016 ms. The accuracy of predictions within kriging and ARIMA for each time series is nearly identical.

Figures 8 and 9 present the values of MAPEs for short (30-day into the future) PMx and PMy prediction using ARIMA and kriging.

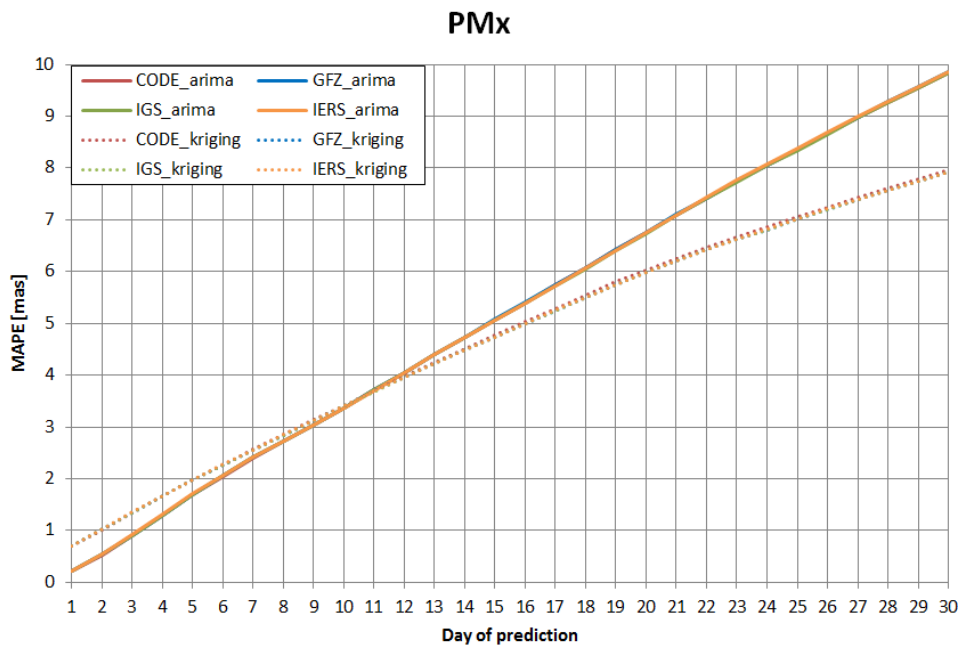


Figure 8. Comparison of MAPEs for 30-day PMx prediction for ARIMA and kriging for various analysis centres

Up to 11 day of PMx prediction, MAPEs for ARIMA are smaller than those for kriging with maximum advantage around 0.5 mas. After this day, kriging reaches better accuracy of forecast. The maximum differences between ARIMA and kriging are on the 30th day and are equal to around 1.91 mas. The accuracy of predictions based on various data centres is nearly identical; the maximum differences vary from around 0.01 mas to 0.05 mas.

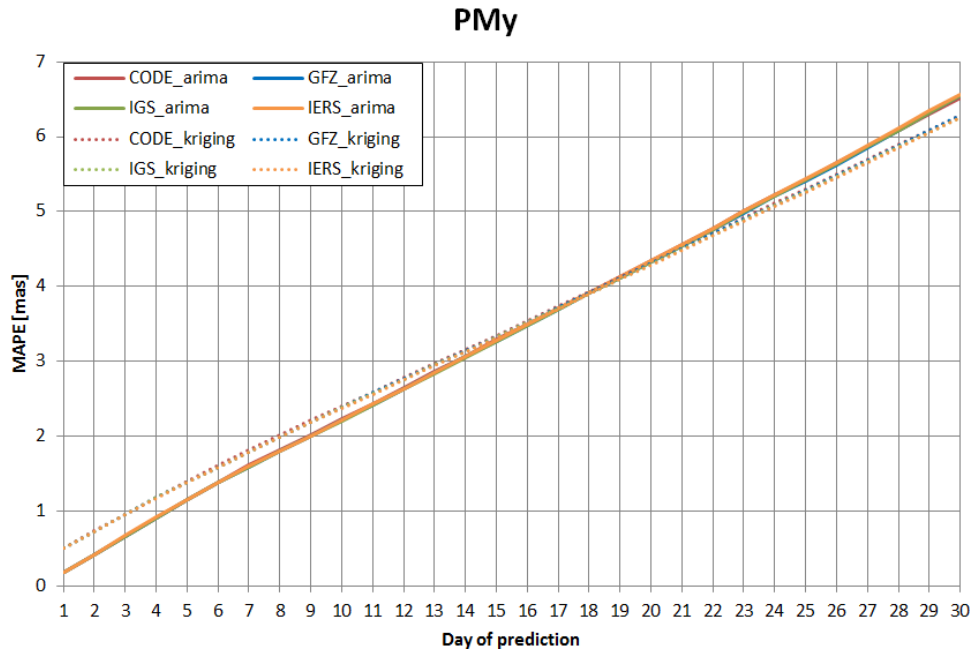


Figure 9. Comparison of MAPEs for 30-day PMy prediction for ARIMA and kriging for various analysis centres

For the first 18 days of PMy prediction, results indicate a better prediction performance of ARIMA model. From the 19th day, the advantage is in favour of kriging and reaches maximum value about 0.3 mas. The differences between predictions based on various data centres are small, around 0.01 – 0.03 mas.

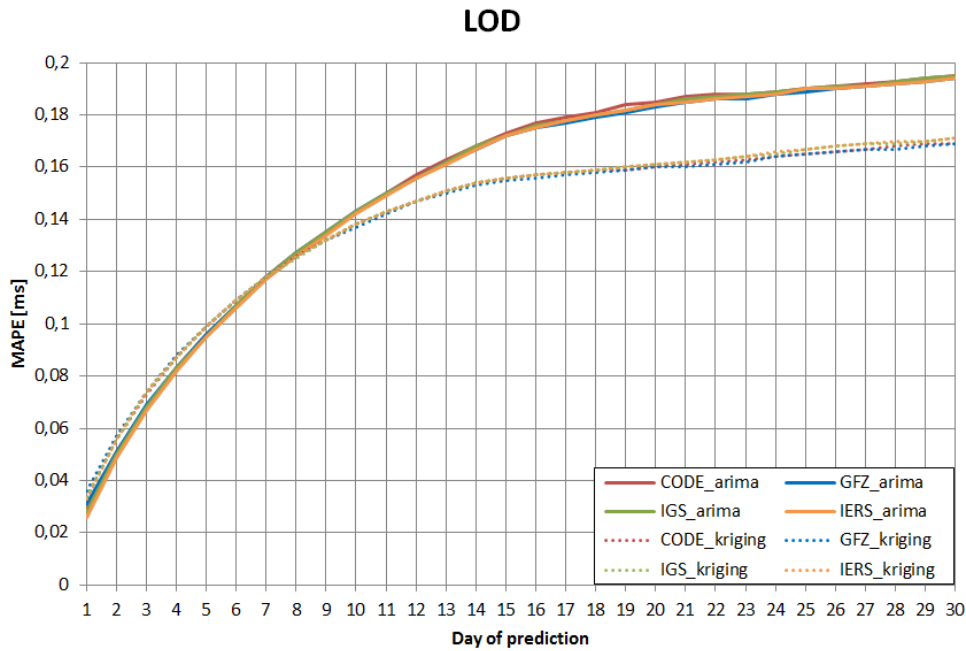


Figure 10. Comparison of MAPEs for 30-day LOD prediction for ARIMA and kriging for various analysis centres

Figure 10 shows a comparison of MAPEs for 30-day LOD prediction for ARIMA and kriging. Results indicate that for the first 6 days, prediction with ARIMA is more accurate. From the 7th day onward, kriging gives a more accurate forecast. The maximum difference between the forecasting methods is about 0.026 ms for CODE (on the last day of prediction). It is worth noting that MAPEs for IGS and IERS using kriging are most similar to each other. In majority, this also holds for ARIMA.

5. CONCLUSIONS

Earth Rotation Parameters predictions based on ordinary kriging and ARIMA model have been presented in this contribution. Predictions have been performed on the basis of rapid (CODE, IGS and GFZ) and final (IERS) ERP products. The quality of polar motion forecast is visibly coordinate-dependent, i.e., PM_x is worse predictable than PM_y. The results indicate that the ARIMA-based prediction is better for ultra-short prediction; for PM_x it turned out to be 11 -days of forecast, for PM_y 18 -days, and for LOD 8 -days. The maximum differences for first few days of 15-day predictions between methods are around 0.32 mas (PM_x), 0.23 mas (PM_y) and 0.004 ms (LOD) in favour of ARIMA. On the last day, the differences reach 0.15 mas (PM_x) and 0.016 ms (LOD) with advantage to kriging. For the first few days of 30-day prediction, ARIMA gives lower MAPEs of approximately 0.5 mas (PM_x), 0.3 mas (PM_y) and 0.007 ms (LOD). The maximum differences of MAPEs on the last days of 30-day predictions are 1.91 mas (PM_x), 0.3 mas (PM_y) and 0.026 ms (LOD) with advantage to kriging method. For all ERP, the differences of MAPEs for time series from various analysis centres are not significant and vary up to maximum value of around 0.05 mas (PM_x), 0.04 mas (PM_y) and 0.005 ms (LOD). These values are on the level of accuracy of corresponding ERP determination, i.e., polar coordinates with the accuracy of app. 50 μ s or better and 10 μ s in case of LOD (Dick and Thaller, 2020). It is also worth noting that the accuracy of prediction on the basis of rapid products (30-day gap filling) is on the same level as on final product only. The conducted comparisons did not give a clear answer as to which method, i.e., ARIMA or kriging, is better for a given ERP and for a given forecast length, with the exception of ultra-short-term (15 days) prediction for PM_y where ARIMA systematically

behaved better. The results of this contribution are supported by a considerable number of performed predictions; therefore, all intermediate results are available at the website mentioned in the acknowledgements section.

Acknowledgements. The paper is a result of research on geospatial methods carried out within the statutory research grant no. 16.16.150.545 at the Department of Integrated Geodesy and Cartography, AGH University of Science and Technology, Krakow.

Intermediate results are available at the website accompanied with this article home.agh.edu.pl/mmichalc.

REFERENCES

- Akaike H., (1998) Information Theory and an Extension of the Maximum Likelihood Principle, In: Parzen, E., Tanabe, K., Kitagawa, G. (eds) Selected Papers of Hirotugu Akaike. *Springer Series in Statistics*, Springer, New York, NY. https://doi.org/10.1007/978-1-4612-1694-0_15
- Akyilmaz O., Kutterer H., Shum C., Ayan T., (2011) Fuzzy-wavelet based prediction of earth rotation parameters, *Applied Soft Computing*, 11(1):837–841, <https://doi.org/10.1016/j.asoc.2010.01.003>
- Box, G.E.P. and Jenkins, G.M. (1976) Time Series Analysis: Forecasting and Control, *Holden Day* San Francisco
- Cressie N.A.C. (1993) Statistics for spatial data, *John Wiley & Sons*, New York
- Dick W. R. and Thaller D. (eds.) IERS Annual Report 2018 (2020) International Earth Rotation and Reference Systems Service, Central Bureau. *Frankfurt am Main: Verlagdes Bundesamts für Kartographie und Geodäsie*, 207 p., ISBN 978-3-86482-136-3
- Dill, R., Dobsław, H., Thomas, M. (2019): Improved 90-day Earth orientation predictions from angular momentum forecasts of atmosphere, ocean, and terrestrial hydrosphere. - *Journal of Geodesy*, 93, 3, pp. 287—295. doi: <http://doi.org/10.1007/s00190-018-1158-7>
- Gambis D, Luzum B., (2011) Earth rotation monitoring, UT1 determination and prediction, *Metrologia*; 48:165-70
- Kalarus M., Schuh H., Kosek W., Akyilmaz O., Bizouard Ch., Gambis D., Gross, B R., Jovanović, Kumakshev S., Kutterer H., Mendes Cerveira P. J., Pasynok S., Zotov L., (2010) Achievements of the Earth Orientation Parameters prediction comparison campaign, *Journal of Geodesy*, 84:587–596
- Kosek W., Kalarus M., Niedzielski T., (2007) Forecasting Of the Earth Orientation Parameters - Comparison of Different Algorithms, *Journées Systèmes de Référence Spatio-temporels*, Observatoire de Paris, 17-19 September 2007
- Kwiatkowski, D., Phillips, P. C. B., Schmidt, P., Shin, Y. (1992) Testing the null hypothesis of stationarity against the alternative of a unit root, *Journal of Econometrics*. 54 (1–3): 159–178, [https://doi.org/10.1016/0304-4076\(92\)90104-Y](https://doi.org/10.1016/0304-4076(92)90104-Y)
- Lei Y., Guo M., Cai H, Hu D., Zhao D., (2015) Prediction of Length-of-day Using Gaussian Process Regression, *The Journal of Navigation*, 68:563–575, <https://doi.org/10.1017/S0373463314000927>
- Liao D.C., Wang Q.J., Zhou Y.H., Liao X.H., Huang C.L., (2012) Long-term prediction of the Earth Orientation Parameters by the artificial neural network technique, *Journal of Geodynamics* Volume 62, Pages 87-92, ISSN 0264-3707,

<https://doi.org/10.1016/j.jog.2011.12.004>

Ligas, M., (2022), Comparison of kriging and least-squares collocation – Revisited, *Journal of Applied Geodesy*, vol. 16, no. 3, 2022, pp. 217-227. <https://doi.org/10.1515/jag-2021-0032>

Linnet. K. (1990). Estimation of the linear relationship between the measurements of two methods with proportional errors. *Statist. Med.*. 9: 1463-1473. <https://doi.org/10.1002/sim.4780091210>

Luo, J., Chen, W., Ray, J., Li J., (2022), Short-Term Polar Motion Forecast Based on the Holt-Winters Algorithm and Angular Momenta of Global Surficial Geophysical Fluids. *Surv Geophys*. <https://doi.org/10.1007/s10712-022-09733-0>

Michalczak M., Ligas M., (2021) Kriging-based prediction of the Earth's pole coordinates, *Journal of Applied Geodesy*, vol. 15, no. 3, pp. 233-241, <https://doi.org/10.1515/jag-2021-0007>

Michalczak M., Ligas M. (2022) The (ultra) short term prediction of length-of-day using kriging, *Advances in Space Research*, <https://doi.org/10.1016/j.asr.2022.05.007>

Modiri S., Belda S., Hoseini M., Heinkelmann R., Ferrándiz J. M., Schuh H., (2020) A new hybrid method to improve the ultra-short-term prediction of LOD, *Journal of Geodesy* 94:23

Nastula J., Chin T. M., Gross R., Śliwińska J., Wińska M., (2020) Smoothing and predicting celestial pole offsets using a Kalman filter and smoother, *Journal of Geodesy* 94:29

Niedzielski T., Kosek W., (2008) Prediction of UT1–UTC, LOD and AAM χ^3 by combination of least-squares and multivariate stochastic methods, *J Geod* 82:83–92

Okhotnikov G., Golyandina N. (2019) EOP Time Series Prediction Using Singular Spectrum Analysis" *RWTH Aachen University*

Passing H. Bablok W.. (1983) A new biometrical procedure for testing the equality of measurements from two different analytical methods. Application of linear regression procedures for method comparison studies in clinical chemistry. Part I. *J Clin Chem Clin Biochem*. Nov;21(11):709-20. doi: 10.1515/cclm.1983.21.11.709. PMID: 6655447

Petit G and Luzum B (eds.). IERS Conventions (2010), IERS Technical Note 36, Frankfurt am Main: Verlag des Bundesamts für Kartographie und Geodäsie. 179 pp., ISBN 3-89888-989-6

Schuh H., Ulrich M., Egger D., Müller J., Schwegmann W. (2002) Prediction of Earth Orientation Parameters by Artificial Neural Networks, *Journal of Geodesy*, 76(5), 247–258, <https://doi.org/10.1007/s00190-001-0242-5>

Wu F., Chang G., Deng K., (2019) One-step method for predicting LOD parameters based on LS+AR model", *Journal of Spatial Science*, 66:2, 317-328, <https://doi.org/10.1080/14498596>

Zotov, Leonid & Bizouard, Ch. (2018). Escargot Effect and the Chandler Wobble Excitation, *Journal of Physics: Conference Series*, 955, 012033, doi: 10.1088/1742-6596/955/1/012033

Received: 2022-07-18

Reviewed: 2022-08-19 (undisclosed name); 2022-08-22 (C. Ron)

Accepted: 2022-10-06